Thioltransferase in Human Red Blood Cells: Kinetics and Equilibrium[†,‡]

John J. Mieyal,* David W. Starke, Stephen A. Gravina,[§] and Barbara A. Hocevar
Department of Pharmacology, Case Western Reserve University School of Medicine, Cleveland, Ohio 44106
Received November 8, 1990; Revised Manuscript Received June 26, 1991

ABSTRACT: Thioltransferase from human red blood cells (HRBC TTase), coupled to GSSG reductase, catalyzed glutathione (GSH)-dependent reduction of prototype substrates hydroxyethyl disulfide (HEDS) and sodium *S*-sulfocysteine as well as of other homo- and heterodisulfides, including the protein mixed disulfide albumin-S-S-cysteine. Whereas apparent K_M values for the substrates varied over more than a 20-fold range, the V_{max} values agreed quite closely, usually within less than a factor of 2, suggesting that initial interaction of oxidized substrate with enzyme is not rate determining. HRBC TTase was inactivated by iodoacetamide (IAA), and this was prevented by pretreatment with disulfides. The pH dependence of IAA inactivation gave a remarkably low apparent pK_a of 3.5, which was independent of ionic strength (0.05–2 M). At pH 6, one radiolabeled carboxyamidomethyl moiety was bound to the enzyme after treatment with [^{14}C]IAA. This unusual thiol reactivity suggests that the active-site cysteine moiety of the TTase may be involved in a hydrogen bond with a carboxylate moiety. In contrast, the pH dependence for GSH-dependent TTase catalysis of disulfide reduction displayed an inflection point near pH 8.0, also suggesting that the initial reaction of oxidized substrate with the active-site thiol is not involved in rate determination. Two substrate kinetic studies of HRBC TTase and rat liver TTase (e.g., [GSH] and [HEDS] varied independently) gave patterns of intersecting lines on double-reciprocal plots ($1/v$ vs $1/S$), indicating a sequential mechanism for the TTase reactions, rather than a ping-pong mechanism. Thus, both GSH and the disulfide substrate appear to interact with the reduced enzyme before the products of disulfide reduction are released, rather than GSH acting simply as a reductant of the oxidized enzyme. When GSSG reductase was omitted, the TTase was shown to catalyze the approach to the same equilibrium position starting from either set of substrates (e.g., GSH + HEDS vs GSSG + β-mercaptoethanol). Thus, TTase action is fully reversible, and the direction of catalysis and extent of reaction depend on the relative concentrations of the respective substrates and on the coupled action of GSSG reductase.

Thioredoxins, thioltransferases, and glutaredoxins comprise a class of low molecular weight enzymes that are capable of catalyzing the reduction of disulfide bonds in a variety of protein and non-protein substrates, and thereby they have been implicated in cellular sulfhydryl homeostatic reactions (Ziegler, 1985; Holmgren, 1985a, 1989; Mannervik et al., 1989). Found throughout nature, these enzymes are classified generally as thiol–disulfide oxidoreductases because thiol groups on the respective enzymes are believed to participate in catalysis. Thus, a characteristic structural feature of these enzymes is an active-site pair of cysteine residues that can exist in oxidized and reduced forms (Stryer et al., 1967; Eriksson et al., 1974; Gan & Wells, 1987). In the oxidized state, thioredoxin and thioltransferase enzymes were shown to be protected against inactivation by thiol reagents like iodoacetate, whereas the reduced enzymes were inactivated with a pH dependence interpreted to reflect the pK_a's of the active-site cysteine moieties in the respective proteins (Kallis & Holmgren, 1980; Gan & Wells, 1987). Although the oxidized forms of all of the enzymes are reducible by DTT,[1] thioltransferases and glutaredoxins are distinguished from thioredoxins by their ability to be reduced by GSH. Moreover, oxidized thioredoxins are recycled by coupling to a specific flavoprotein, thioredoxin reductase, that does not reduce thioltransferase and glutaredoxin, whereas the thioltransferase and glutaredoxin enzymes are recycled by coupling to GSH and GSSG reductase that does not recycle thioredoxin. Thioredoxins have been distinguished also by amino acid sequences that show essentially no homology with the thioltransferase and glutaredoxin proteins, although the global conformations of thioredoxin and glutaredoxin are considered to be similar according to X-ray data and modeling studies (Holmgren, 1989). A high degree of homology has been noted among a number of the glutaredoxin and thioltransferase sequences (Papayannopoulos et al., 1989), leading to the supposition that thioltransferase and glutaredoxin may be alternative names for the same set of enzymes (Mannervik et al., 1989).

Mechanisms for the catalysis of disulfide reduction by thioredoxin (Kallis & Holmgren, 1980) and thioltransferase (Gan & Wells, 1987) have been proposed whereby the intramolecular disulfide form of the respective enzyme would

[†] This work was supported in part by grants from the Northeast Ohio Affiliate and the National Center (No. 881186) of the American Heart Association and by grants from the National Institute on Aging (AG-04391-08) and the American Cancer Society, Cuyahoga County Unit. The results of this study were presented in part at the Annual FASEB Meeting, Washington D.C., April 1990. This is a publication of the Protein Group at Case Western Reserve University.

[‡] This article is dedicated to Leslie T. Webster, Jr., on the occasion of his 65th birthday.

* Author to whom correspondence should be addressed.

[§] Part of this study was conducted by Stephen A. Gravina in partial fulfillment of the requirements for the Ph.D. degree, Case Western Reserve University.

[1] Abbreviations: $CSSO_3$, sodium *S*-sulfocysteine; DTT, dithiothreitol; EDTA, ethylenediaminetetraacetic acid; G-6-PD, glucose-6-phosphate dehydrogenase; GRx, glutaredoxin; GSH, glutathione; GSSG, oxidized glutathione; HEDS, hydroxyethyl disulfide; HEPES, *N*-(2-hydroxyethyl)piperazine-*N*′-2-ethanesulfonate; Hb, hemoglobin; HRBC, human red blood cell; IAA, iodoacetamide; β-ME, β-mercaptoethanol; MES, 2-(*N*-morpholinoethane)sulfonate; RBC(s), red blood cell(s); TRx, thioredoxin; TTase, thioltransferase; CoA-S-SG, coenzyme A-glutathione disulfide.

0006-2960/91/0430-8883$02.50/0

be an intermediate in the overall reaction after formation of the reduced product(s) of the disulfide substrate; the enzyme would then be reduced to complete the cycle. Such mechanisms would be expected to generate a ping-pong kinetic pattern for the reactions of each enzyme, but two-substrate kinetic studies have not been reported for these enzymes. Although the concept of catalysis of reversible thiol–disulfide interchange reactions by these enzymes is implicit in their name, they have generally been presented as catalysts of disulfide reduction (Ziegler, 1985; Holmgren, 1985a, 1989; Mannervik et al., 1989).

We isolated an enzyme from human erythrocytes that has characteristics identifying it as a thioltransferase (glutaredoxin), and it catalyzed several reactions in vitro that suggest that it may play an important role in sulfhydryl homeostasis in RBCs (Mieyal et al., 1991). This article is focused on aspects of the mechanism of TTase catalysis. Distinction between the apparent pK_a values for active-site thiol modification (pH 3.5) and overall catalysis (pH 8.0) as well as coincident V_{max} values for a variety of disulfide substrates indicate that a reactive SH moiety is poised for initiating disulfide reduction catalysis, but this first step is not involved in rate determination. Two substrate kinetic patterns for the disulfide reduction reaction suggest a sequential mechanism for TTase rather than a ping-pong mechanism as previously suggested. In the absence of GSSG reductase, the HRBC TTase catalyzes both GSH-dependent disulfide reduction and GSSG-dependent thiol oxidation leading to the same equilibrium position.

Experimental Procedures

Materials. NADPH was purchased from Boehringer Mannheim. Ammonium sulfate, coenzyme A disulfide, coenzyme A–glutathione disulfide (CoA-S-SG), *S*-cysteinyl-albumin, β-mercaptoethanol, dithiothreitol, EDTA (disodium), glutathione (reduced and oxidized), cysteine, L-cystine, iodoacetamide, sodium acetate, glycylglycine, MES, HEPES, Tricine, and Tris base were obtained from Sigma. K_2HPO_4 and KH_2PO_4 (≤0.0004% Fe) were obtained from Fisher. [^{14}C]Iodoacetamide (23 nCi/nmol) was obtained from ICN. Glutathione reductase (from yeast or from bovine intestinal mucosa; activity for CoA-S-SG ≤ 30% of the activity for GSSG) was acquired from U.S. Biochemicals and Sigma. Glutathione reductase (from spinach; activity for CoA-S-SG < 0.5% of the activity for GSSG) was purchased from Sigma. *S*-Sulfocysteine (sodium salt) was synthesized according to the procedure of Segel and Johnson (1963) and then recrystallized twice from aqueous ethanol and dried in vacuo before use. All other chemicals and solvents were reagent grade from standard sources.

Standard Assay for Thioltransferase Activity. One milliliter of aqueous reaction mixture contained 0.2 mM NADPH, 0.5 mM GSH, 0.1 M potassium phosphate buffer, pH 7.5, 2 units of GSSG reductase, and 2 mM HEDS. Separate concentrated stock solutions of the assay components were stored frozen (−70 °C). Iron-free potassium phosphate was used for the assay buffer, and it was confirmed by separate experiments that added EDTA (5 mM) showed no effect on the assay of TTase activity. GSH, NADPH, and potassium phosphate were mixed, diluted with the appropriate proportions of water and thioltransferase enzyme solution (total volume 0.9 mL), and preincubated in the spectrophotometer for 5 min at 30 °C before the reaction was initiated with 0.1 mL of 20 mM HEDS. Prior to HEDS addition there was no difference between the spectrophotometer traces for the corresponding samples with and without TTase, indicating that the TTase preparations used were free from any GSH- and NADPH-oxidase activities. After HEDS addition, the slope of the linear portion of the time course of decreasing A_{340nm} for the minus TTase control was subtracted from the slopes of the TTase-containing samples in order to determine the TTase-dependent rates. In separate experiments it was confirmed that GSSG reductase was not limiting and that there was a 1:1 correspondence between GSSG production and NADPH utilization. One unit of TTase activity is defined as 1 μmol of NADPH oxidized/min (i.e., A_{340nm} for NADPH = 6.2 mM^{-1} cm^{-1}) under these standard assay conditions.[2]

Preparation of HRBC Thioltransferase. The procedure for purification of HRBC TTase was described previously (Mieyal et al., 1991). Usually partially purified TTase (3–4 units/mg of protein) was used for the kinetic studies, but separate experiments verified that there were no differences in the kinetic data when fully purified TTase was used.

Preparation of Rat Liver Thioltransferase. To prepare a small quantity of TTase for comparative kinetic studies, livers were removed from five Sprague-Dawley (400-g) rats. Partial purification was performed by proportionately scaling down a published procedure through the stage of ammonium sulfate fractionation (Gan & Wells, 1986). Activity of this preparation (0.7 unit/mL) was determined by our standard TTase assay procedure (Mieyal et al., 1991).

Assays of Substrate Concentration Dependence. The oxidized substrates, whose concentrations were varied, were substituted for HEDS in the standard thioltransferase assay mixture containing 0.08 unit of TTase. Concentrations of the individual substrates were varied through appropriate ranges, which were limited by such variables as solubility, high nonenzymic rates of reaction with GSH, or substrate inhibition of the TTase-catalyzed reaction. Estimates of apparent K_M and V_{max} values were obtained by nonlinear least-squares analysis, utilizing Simplex algorithm fitting to the Michaelis–Menten equation (Caceci & Cacheris, 1984).

Iodoacetamide Inactivation Kinetics. Thioltransferase (0.01 unit) was added to two sets of solutions (10-μL total volume) at 25 °C containing 0.15 M Tris-HCl, pH 8.8, 10–50 μM DTT (to ensure that the TTase active-site dithiol was fully reduced),[3] and various concentrations of IAA. Each sample from one set was processed immediately (zero time); the corresponding sample from the other set was processed after 5 min of incubation as follows. Each reaction mixture was diluted to 1 mL (100-fold) with standard assay mixture in order to quench the IAA reaction, and the TTase activity was measured spectrophotometrically (as described above). The concentration dependence of IAA inactivation of thioltransferase was analyzed according to a modification of the expression derived by Kitz and Wilson (1962). We simplified the approach by using a single time of preincubation of TTase enzyme with each concentration of inactivator (IAA) rather than generating

[2] We have also monitored thioltransferase activity routinely with *S*-sulfocysteine (sodium cysteinethiosulfate) as the non-glutathione substrate. In this case the standard assay was the same as described above except that 2 mM HEDS was replaced by 1 mM $CSSO_3$ and the reactions were run at 25 °C. Under these conditions a given amount of enzyme displays essentially the same rate of NADPH oxidation in the coupled assay as with the HEDS assay.

[3] The concentration of DTT was varied somewhat depending on the preparation of TTase being used for the experiments. Complete inhibition after preincubation of the TTase for 10 min with 200 μM IAA at pH 8 was used as the criterion for complete reduction of the TTase by DTT. No differences were observed in the concentration dependence or pH dependence of IAA inactivation with several preparations of TTase at different stages of purity [post-phenyl-Sepharose to post-hydroxylapatite (Mieyal et al., 1991)] treated with DTT up to 50 μM.

a complete kinetic curve to obtain $t_{1/2}$ at each [IAA]. This approach was validated by demonstrating that pseudo-first-order kinetics were obeyed over a time course encompassing the fixed time point (5 min in this case), at the extremes of the IAA concentration range. K_I and k_{inact} were determined by nonlinear regression analysis of the relationship between enzyme activity remaining at time t and inactivator concentration, according to the following expression that describes a typical rectangular hyperbolic relationship:

$$\ln (E_0/E_t)/t = k_{inact}[I]/K_I + [I]$$

where E_0 and E_t represent the enzymatic activity at times 0 and t (5 min), respectively, [I] refers to the concentration of inactivator (IAA), K_I is the concentration of inactivator that gives half the maximal rate of inactivation, and k_{inact} is the net rate constant of inactivation. This expression can be rearranged to give a linear double-reciprocal plot (t/ln (E_0/E_t) vs 1/[I]).

Dependence of IAA Inactivation of pH. Samples of TTase were treated with IAA and assayed as described above, except that various buffers at various pH values were substituted for the Tris buffer. Ionic strength was maintained constant at 0.055, 0.3, or 2 M by addition of appropriate amounts of NaCl. The preincubation period with IAA was 3 min, and the IAA concentration was fixed at 300 μM. In separate experiments, it was confirmed that the inactivation of TTase followed pseudo-first-order kinetics throughout the pH range tested, and that the 3-min point was on the linear portion of the ln (TTase activity) vs time curves.

Stoichiometry of [^{14}C]Iodoacetamide Radiolabeling. Samples of pure HRBC TTase (5 μg) were incubated at room temperature in 50-μL reaction mixtures containing 50 μM DTT and 300 μM [^{14}C]IAA in 10 mM MES buffer, pH 6.0. The reactions were initiated by adding concentrated [^{14}C]IAA. At 20 min, 50 μL of 20 mM unlabeled IAA was added, and the mixtures were either dialyzed against multiple changes of 10 mM potassium phosphate, pH 7.5 (until no radioactivity appeared in the dialysis buffer), or placed on hydrated nitrocellulose in a Hybri-slot manifold (BRL Corp.) to bind the protein, and then washed extensively with 1 M potassium phosphate (pH 7.5) to remove unreacted [^{14}C]IAA. In the latter case, parallel mixtures were processed that contained no TTase in order to control for nonspecific binding of radioactivity. After dialysis, protein concentration was determined by BCA analysis as described (Mieyal et al., 1991) and radioactivity was determined by liquid scintillation counting (Beckman LS 5000 CE). Individual pieces were cut from the nitrocellulose corresponding to individual samples, and these were placed in liquid scintillant (Bio-safe II, RPI Corp.) for quantitation of radioactivity. Irreversible association of radioactivity with the protein was indicative of carboxyamidomethylation of cysteine on TTase, and the stoichiometry (nanomoles of [^{14}C]NH_2COCH_2-S per nanomole of TTase) was calculated from the specific radioactivity of [^{14}C]IAA (23 nCi/nmol) and the MW of TTase (11 300 ng/nmol; Mieyal et al., 1991). The two methods of processing the samples gave indistinguishable results.

Two-Substrate Kinetics. Substrates (GSH and HEDS, or GSH and $CSSO_3$) were independently varied to produce a 4 × 4 matrix of concentration sets (n = 4). Either HRBC TTase or rat liver TTase was added to all mixtures at a constant concentration (within the linear range of enzyme concentration dependence, determined separately). Each individual data set for a varied substrate at a fixed concentration of the complimentary substrate was analyzed by nonlinear least-squares analysis as described above. The individual sets of data were presented in composite format as patterns of double-reciprocal plots (Figures 3 and 4) to facilitate interpretation.

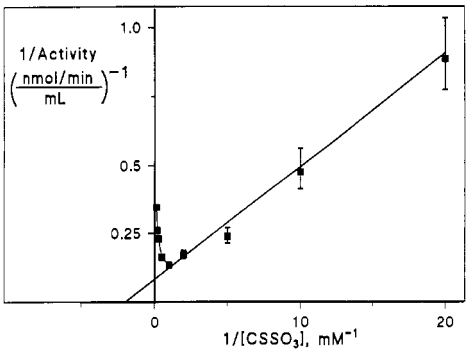

FIGURE 1: Dependence of HRBC thioltransferase activity on *S*-sulfocysteine concentration. All reactions were run in 1 mL at 25 °C, 0.1 M potassium phosphate, pH 7.5/0.2 mM NADPH/0.5 mM GSH/2 units of GSSG reductase/0.008 unit of HRBC TTase (see Experimental Procedures). The *S*-sulfocysteine concentration was varied as indicated, and the data are presented in double-reciprocal format. Each point represents the mean of at least three separate experiments ± SE.

Table I: Kinetic Parameters of Typical Oxidized Substrates for HRBC Thioltransferase[a]

substrate	K_M(app)[b] (mM)	V_{max} (turnover no.)[c] (min^{-1})
S-sulfocysteine	0.39	1200
L-cystine	0.16	1500
hydroxyethyl disulfide	0.73	1420
coenzyme A disulfide	3.44	840
CoA-glutathione mixed disulfide	0.27	1830
S-cysteinylalbumin mixed disulfide	0.22	1080

[a] All reactions were run in 1 mL at 25 °C, 0.1 M potassium phosphate, pH 7.5/0.2 mM NADPH/0.5 mM GSH/2 units of GSSG reductase/0.008 unit of HRBC TTase (see Experimental Procedures). [b] K_M(app) was calculated by nonlinear fit of the velocity vs [substrate] data, as described under Experimental Procedures. In most cases at least four concentrations of substrate were included in the analysis and at least six separate experiments were conducted. For the CoA substrates, at least three separate experiments were run. Most of the oxidized substrates displayed substrate inhibition at high concentrations, so estimates of K_M and V_{max} were determined from the range of concentrations where inhibition was not evident (i.e., the linear region of $1/v$ vs $1/S$ plots). In all cases the highest concentration of substrate included in the calculation of the kinetic parameters was $\geq 2K_M$. [c] Turnover numbers were calculated by dividing the V_{max} values by the specific activity (110 units/mg) and molecular weight (11 300 μg/μmol) of pure TTase (Mieyal et al., 1991).

Results

Kinetic Evaluation of Typical Oxidized Substrates for HRBC TTase. The dependence of HRBC TTase activity on the concentration of *S*-sulfocysteine displayed substrate inhibition at higher concentrations (Figure 1). This behavior was typical of all of the oxidized substrates that were tested (Table I). Consequently, values of V_{max} and K_M were estimated in each case from the concentration range where substrate inhibition was not evident. As illustrated, this range was 0.05–1 mM for *S*-sulfocysteine (Figure 1); i.e., $0.13K_M$–$2.6K_M$. For these studies the GSH concentration was maintained constant at 0.5 mM. Although not saturating for GSH (see two-substrate kinetics, below), this concentration kept the rates of spontaneous reaction between GSH and the oxidized substrates low relative to those of the TTase-catalyzed reactions.

Like the thioltransferases isolated from the livers of other mammals, coupled to GSSG reductase, the human RBC

thioltransferase displayed broad substrate reactivity in catalyzing the reduction of a variety of small disulfide compounds as well as the protein mixed disulfide cysteinylalbumin (Table I). Whereas the apparent K_M values varied over more than a 20-fold range, the V_{max} values (expressed as turnover numbers) for the various substrates agreed more closely, usually within less than a factor of 2. This similarity in V_{max} values suggests that the rate-determining step for these reactions occurs subsequent to the initial interaction of the oxidized substrate with the TTase enzyme (see Discussion).

Inhibition of HRBC TTase by IAA. HRBC TTase was inactivated in a time- and concentration-dependent manner by iodoacetamide. In separate experiments the time courses of inactivation of TTase by IAA reflected first-order kinetics (linear ln [TTase activity remaining] vs time curves; data not shown). The IAA concentration dependence of TTase inactivation (resulting from 5 min of preincubation of TTase with various concentrations of IAA; see Experimental Procedures) obeyed a typical rectangular hyberbolic relationship ($\ln (E_0/E_t)/t = k_{inact}[I]/K_I + [I]$). Nonlinear regression analysis of the data (at least three determinations of E_0 and E_t at each of six IAA concentrations from 50 to 300 μM) gave values for k_{inact} = 1.1 min^{-1} and K_I = 300 μM. These results are consistent with covalent modification of the enzyme preceded by reversible IAA–TTase complex formation as depicted in the reaction scheme below, where $k_2 < k_{-1}$ and E* represents the covalently inactivated TTase enzyme after displacement of iodide (I^-):

$$E + IAA \underset{k_{-1}}{\overset{k_1}{\rightleftharpoons}} E\text{–}IAA \xrightarrow{k_2} E^* + I^-$$

Protection against IAA inhibition by pretreatment with disulfide substrates is diagnostic of the thiol–disulfide oxidoreductase family of enzymes with their active-site pairs of cysteine residues. When HRBC TTase was preincubated with HEDS or cystine and the disulfide substrate was then diluted or removed by dialysis, the resulting enzyme was unaffected by concentrations of IAA > ($10K_I$) (data not shown). The concentration dependence of the protective effect of cystine ($K_{protect}$ = 70 μM) was similar to that for cystine as substrate (K_M = 160 μM; Table I).

Because the reaction of thiols with IAA is favored by deprotonation of the thiol to the thiolate anion, we examined the pH dependence of the IAA inactivation of HRBC TTase (Figure 2). A typical sigmoid titration curve of TTase activity remaining vs pH was obtained, which gave a pK_a = 3.5 for the inactivation reaction. The shape and position of the curve was found to be independent of the nature of the buffers used and independent of ionic strength over the range 0.05–2 M. Because IAA itself has no ionizable groups, this pH dependence is attributed to the TTase enzyme and presumably involves the active-site cysteinyl moiety. Consistent with this interpretation, about one radiolabeled carboxyamidomethyl moiety (0.90 ± 0.02; n = 3) was incorporated into the enzyme when it was incubated for 20 min at pH 6 with [^{14}C]IAA (see Discussion).

Optimum pH for HEDS Reduction in the GSSG Reductase Coupled HRBC TTase System. The pH-dependent variation of HRBC TTase-catalyzed reduction of HEDS displayed a typical titration curve with an inflection point near pH 8.0 (Figure 2, right; upper curve). The spontaneous reaction of GSH and HEDS displayed a similar pH dependence (lower curve). The distinct separation between the apparent ionization of the active-site cysteine (Figure 2) and the pH optimum for catalysis suggests that reaction of disulfide substrate with the cysteine thiol moiety is not involved in the rate-determining step of the overall reaction (see Discussion).

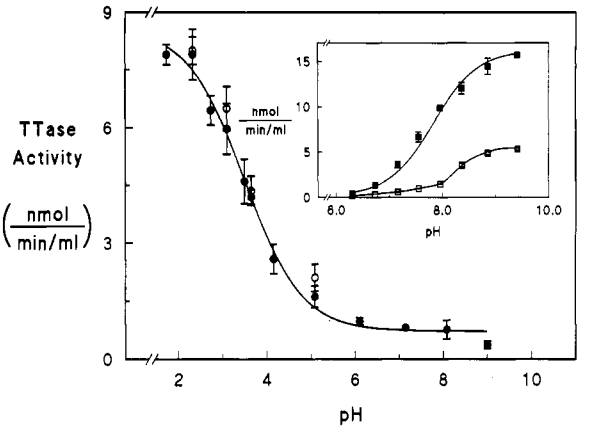

FIGURE 2: Dependence of TTase inactivation by IAA on pH and ionic strength. Preincubation of thioltransferase (0.01 unit) with 300 μM IAA in various buffers at different pH values (see below) was carried out for 3 min at room temperature. All buffers were 0.04 M, and ionic strength was maintained at 0.055 M (solid symbols), 0.3 M (data not shown), or 2 M (open symbols) by the addition of appropriate amounts of NaCl. The data for 0.3 M ionic strength overlapped those shown but are not included in order to avoid clutter. After preincubation, the reaction mixtures were diluted 100-fold into standard assay mixtures and assayed for TTase activity as described under Experimental Procedures. The following buffers were used: sodium acetate (pH 3.5–5.0); glycylglycine (pH 2.0–3.5); MES (pH 6.0); HEPES (pH 7.0); and Tricine (pH 8.0–9.0). (Inset) Dependence of TTase activity and spontaneous GSH-dependent HEDS reduction on pH. The rate of formation of GSSG was measured in the absence and presence of HRBC TTase (0.01 unit) by the standard coupled assay system with HEDS and GSH at 30 °C except that 0.1 M potassium phosphate buffer, pH 7.5, was replaced by a number of buffers at the pH values indicated. Sufficient GSSG reductase was added at each pH condition to ensure that its activity was not limiting. The buffer concentration in all cases was 0.04 M, and ionic strength was maintained constant at 0.3 M by addition of appropriate amounts of KCl. The different buffers were overlapped with respect to pH values: MES, pH 6.0–6.5; HEPES, pH 6.5–8.0; and Tricine, pH 8.0–9.5. The solid symbols refer to the TTase-mediated reaction *after* subtraction of the nonenzymic rates (open symbols).

Two-Substrate Kinetics for HRBC TTase. Figure 3A,B displays the kinetic patterns that were obtained when the dependence of TTase activity on the concentration of HEDS was studied as a function of GSH concentration and vice versa. The intersecting lines on the double-reciprocal plots are indicative of a sequential mechanism for the HRBC TTase reaction. Similar patterns were obtained when *S*-sulfocysteine ($CSSO_3$) was used as the oxidized substrate rather than HEDS (data not shown). In addition, we observed analogous kinetic patterns for rat liver TTase (Figure 4A,B). As a positive control to validate use of the coupled assay system for these two-substrate kinetic studies, we substituted glutathione peroxidase and H_2O_2 for TTase and HEDS. Glutathione peroxidase catalyzes an analogous redox reaction that generates GSSG, and previous two-substrate kinetic studies using a different assay system gave patterns of parallel lines on double-reciprocal plots indicative of a ping-pong mechanism (Flohe & Gunzler, 1974). Our two-substrate kinetic data for glutathione peroxidase, using the coupled assay, generated the expected pattern of parallel lines for independent variation of GSH and H_2O_2 (data not shown).

TTase Catalysis of Reversible Thiol–Disulfide Interchange: Approach to Equilibrium. Under normal continuous assay conditions with GSSG reductase present, a linear time course was established, after a short lag phase, that proceeded to nearly complete oxidation of the NADPH present (i.e., 200 nmol). Without GSSG reductase, the reduction of HEDS, $CSSO_3$, or cystine essentially stopped after the accumulation

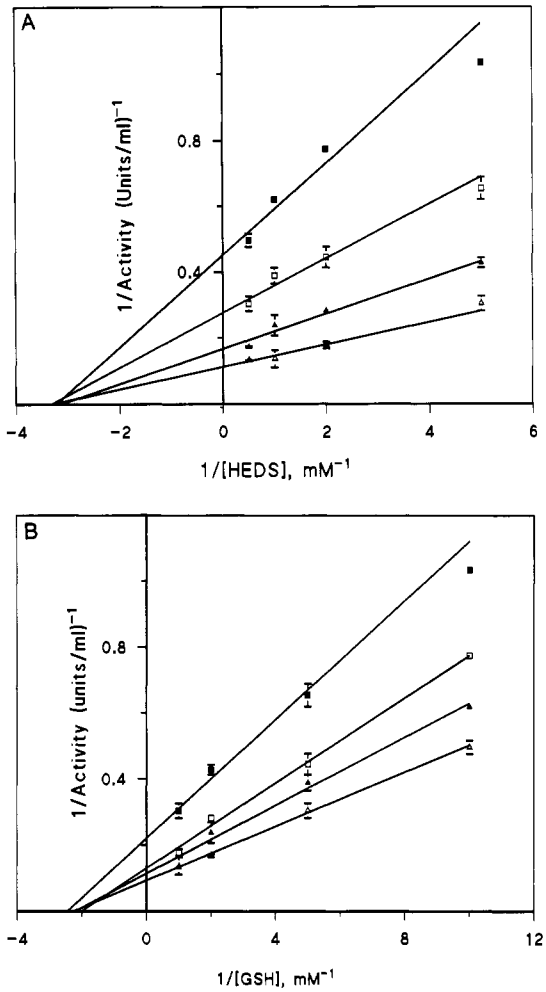

FIGURE 3: Two-substrate kinetic patterns for HRBC thioltransferase: (A) dependence of TTase activity on [HEDS] at various GSH concentrations; (B) dependence of TTase activity on [GSH] at various HEDS concentrations. HRBC thioltransferase activity (0.009 unit under standard assay conditions) was studied as a function of varying GSH and HEDS concentrations. Activity was assayed spectrophotometrically according to the standard coupled system with 0.2 M NADPH and 2 units of GSSG reductase at 25 °C in 1-mL total volume of 0.1 M potassium phosphate, pH 7.5, except that the HEDS and GSH concentrations were varied as shown in the figures and indicated below. (A) The GSH concentrations were as follows: 0.1 mM (closed rectangles); 0.2 mM (open rectangles); 0.5 mM (closed triangles); 1.0 mM (open triangles). (B) The HEDS concentrations were as follows: 0.2 mM (closed rectangles); 0.5 mM (open rectangles); 1.0 mM (closed triangles); 2.0 mM (open triangles). Each data point represents the mean of at least three separate experiments ± SE.

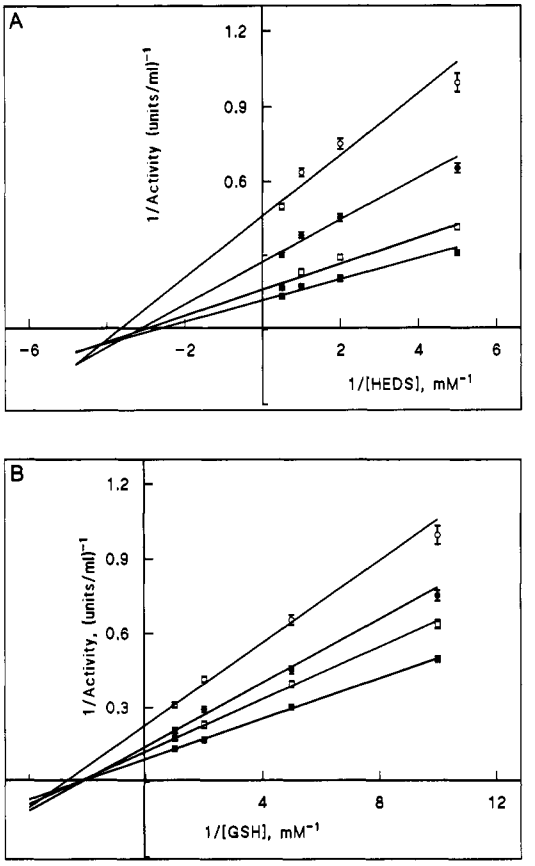

FIGURE 4: Two-substrate kinetic patterns for rat liver thioltransferase: (A) dependence of TTase activity on [HEDS] at various GSH concentrations; (B) dependence of TTase activity on [GSH] at various HEDS concentrations. Rat liver thioltransferase activity (0.023 unit under standard assay conditions) was studied as a function of varying GSH and HEDS concentrations. Activity was assayed spectrophotometrically according to the standard coupled system with 0.2 M NADPH and 2 units of GSSG reductase at 30 °C in 1-mL total volume of 0.1 M potassium phosphate, pH 7.5, except that the HEDS and GSH concentrations were varied as shown in the figure and indicated below. (A) The GSH concentrations were as follows: 0.1 mM (open circles); 0.2 mM (closed circles); 0.5 mM (open rectangles); 1.0 mM (closed rectangles). (B) The HEDS concentrations were as follows: 0.2 mM (open circles); 0.5 mM (closed circles); 1.0 mM (open rectangles); 2.0 mM (closed rectangles). Each data point represents the mean of at least three separate experiments ± SE.

of GSSG that amounted to the equivalent of much less than 50% oxidation of the available NADPH (assayed by adding GSSG reductase after various times of preincubation of the substrates ± TTase). Originally interpreted as indicative of potent product inhibition by GSSG (Holmgren, 1979, 1985b), this phenomenon more likely represents the approach to equilibrium. Thus, the initial rate of GSH-dependent HEDS reduction by HRBC TTase without GSSG reductase was about the same as that observed in the coupled assay system with the reductase (Table II). Also, the same end point of GSSG production from the reaction of GSH and HEDS was approached in the presence or absence of TTase, even though the mechanisms of the spontaneous and TTase-mediated reactions are different. For comparison the reaction of GSH and cystine was also tested. Although a different amount of GSSG was produced relative to the HEDS reaction, again the initial rates in the absence and presence of GSSG reductase were comparable (Table II), and the same end point was approached for the spontaneous and TTase-catalyzed reactions.

Table II: Rates of Reduction of Disulfides by TTase ± GSSG Reductase (GRase)[a]

GSH + HEDS	initial rate[b] (nmol/min)	GSH + cystine	initial rate[b] (nmol/min)
+TTase, −GRase	4.4 ± 0.3	+TTase, −GRase	2.2 ± 0.5
+TTase, +GRase	5.0 ± 0.5	+TTase, +GRase	2.7 ± 0.5

[a] All reactions were run in 1 mL at 30 °C, 0.1 M potassium phosphate, pH 7.5/0.2 mM NADPH/0.5 mM GSH/2 mM HEDS or 1 mM cystine as indicated; 2 units of GSSG reductase was added initially or after preincubation of the other components for specific periods of time. HRBC TTase (0.005–0.015 unit) was added as indicated. All data represent the mean ± SE of 3–6 separate experiments. [b] The initial rate was calculated from the difference between the values of ΔA_{340nm} obtained after the addition of GSSG reductase to mixtures of substrates that were incubated at 30 °C for 1 min in the absence and presence of TTase, without GSSG reductase (line 1) or from the difference in slopes of the spectrophotometric traces (ΔA_{340nm}/min) for the continuous GSSG reductase-coupled assay of the GSH–HEDS or GSH–cystine reactions in the absence and presence of TTase (line 2).

Unequivocal evidence for TTase catalysis of both the forward and reverse reactions toward equilibrium is shown in

Figure 5. In the absence of NADPH and GSSG reductase, mixtures of HEDS and GSH or β-mercaptoethanol and GSSG progressed to the same end point concentration of GSSG, and HRBC TTase accelerated the approach in each direction: HEDS + 2GSH ⇌ 2β-ME + GSSG. As expected, essentially the same value for the equilibrium constant was calculated from the respective end point concentrations when different initial concentrations of reactants were used (see legend to Figure 5).

Discussion

Substrate Selectivity of the Thioltransferase-Like Enzymes. HRBC TTase displayed a broad substrate reactivity (Table I) reminiscent of other mammalian TTases (glutaredoxins) (Ziegler, 1985). This broad reactivity might simply reflect the matching of redox potentials of the various substrates with those of the respective enzymes, where redox potential differences may contribute more than differences in substrate binding sites to observed differences in apparent K_M values. Alternatively, the superfamily of thiol–disulfide oxidoreductase enzymes might be analogous to the cytochrome P-450 superfamily where the isoenzymes have a common active-site domain (thiolate-ligated heme) and overlapping substrate activities, yet a high degree of selectivity for particular substrates is displayed by certain P-450 isozymes (Guengerich, 1990), probably reflecting specific active-site determinants of molecular recognition. Some indications of differential efficiency or substrate preference are notable among the thiol–disulfide oxidoreductase enzymes that have dicysteine active sites in common. For example, the *Escherichia coli* glutaredoxin system is about 10 times more efficient than the thioredoxin system for the ribonucleotide reductase reaction (Holmgren, 1989), and *E. coli* thioredoxin is better than *E. coli* glutaredoxin or rat liver TTase in catalyzing reductive denaturation of insulin (Mannervik et al., 1983). In a model study of oxidative stress to heart cells, *E. coli* thioredoxin did not reactivate creatine kinase, but it readily catalyzed the reactivation of phosphorylase *b* (Park & Thomas, 1989). HRBC TTase displays broad reactivity with prototype substrates (Table I), and it catalyzes reduction of the RBC-specific substrate Hb-S-S-G (Mieyal et al., 1991). It remains to be seen, however, whether the various thiol–disulfide oxidoreductase enzymes may be distinguishable according to differences in substrate selectivity, possibly related to tissue-specific differences in the substrate recognition sites on the respective enzymes.

Reaction Mechanism. A common feature of all thiol–disulfide oxidoreductase enzymes whose amino acid sequences are known is a pair of cysteine residues separated by two intervening amino acids at the active site. The reactivity of these enzymes has been attributed to stabilization of the thiolate anion form of one of these Cys residues (e.g., Cys-32 in *E. coli* thioredoxin; Cys-22 in pig liver TTase) presumably by neighboring cationic residues. According to a prevalent view of the catalytic mechanism (Holmgren, 1985a; Gan & Wells, 1987), the first Cys moiety in its thiolate anion form facilitates nucleophilic reaction with the disulfide substrate; the second Cys then forms an intramolecular disulfide intermediate that must be reduced by GSH (or thioredoxin reductase). This mechanism would predict ping-pong kinetics for the relationship between RSSR′ and GSH (or thioredoxin reductase) as substrates (see below).

Stabilization of the Thiolate Anion and Its Role in Catalysis. Inactivation and labeling of *E. coli* thioredoxin by [^{14}C]IAA followed a pH profile consistent with deprotonation of the Cys-32 SH group with a pK_a of 6.7 (Kallis & Holmgren,

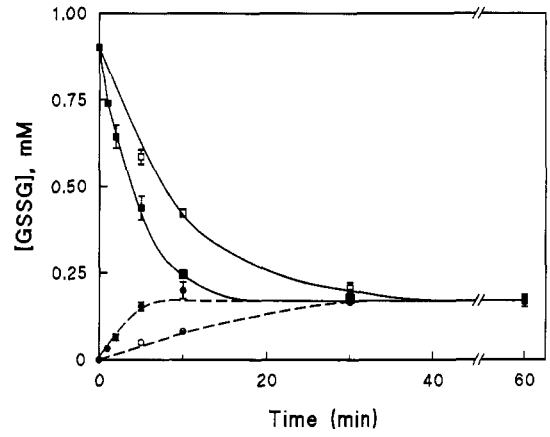

FIGURE 5: TTase catalysis of reversible thiol–disulfide interchange—approach to equilibrium. All reactions were run in 2.2 mL at 30 °C, 0.091 M potassium phosphate, pH 7.5. For one set of experiments (lower lines in the figure) the initial reaction mixtures also contained 0.91 mM HEDS and 1.82 mM GSH, ±HRBC TTase (0.01 unit); for the other set of experiments (upper lines in the figure) 0.91 mM GSSG and 1.82 mM β-ME were included, ±HRBC TTase (0.01 unit). The solid symbols in each case refer to the "plus TTase" data; the open symbols depict "minus TTase" data. Separate stock solutions of the reactants were prewarmed to 30 °C, and each reaction was initiated by adding the reduced substrate (β-ME or GSH). At the time points indicated, 0.2 mL of each resultant reaction mixture was withdrawn and added to 0.8 mL of 0.25 mM NADPH in 0.125 mM potassium phosphate, pH 7.5; after mixing and reading an initial A_{340nm} value, 2 units of GSSG reductase was added and the decrease in A_{340nm} was monitored until it reached a plateau (ca. 2 min). Total GSSG was calculated from the values of ΔA_{340nm} (1 nmol/$0.005\Delta A_{340nm}$, determined from a separate standard curve for authentic GSSG). All data points represent the mean ±SE of two separate experiments. Calculation of equilibrium constants and redox potential: shown below are the calculations of the concentrations of the reactants at equilibrium (data from Figure 5). In separate experiments, 2.0

$$[GSSG]_{obsd} = 175 \times 10^{-6}\ M$$

$$[\beta\text{-ME}] = 2[GSSG] = 350 \times 10^{-6}\ M$$

$$[HEDS]_f = [HEDS]_i - [GSSG] = (909 - 175) \times 10^{-6}\ M = 734 \times 10^{-6}\ M$$

$$[GSH]_f = [GSH]_i - 2[GSSG] = (1818 - 350) \times 10^{-6}\ M = 1468 \times 10^{-6}\ M$$

$$K_{eq} = \frac{[GSSG][\beta\text{-ME}]^2}{[HEDS][GSH]^2} = \frac{(175)(350)^2}{(734)(1468)^2} = 1.36 \times 10^{-2}$$

mM HEDS and 2.0 mM GSH were combined as described above (Figure 5) and incubated for >60 min; the final [GSSG] observed was 240 μM. This value gave the same equilibrium constant (shown below), as expected. The estimation of redox potential is also shown

$$K_{eq} = \frac{[GSSG][\beta\text{-ME}]^2}{[HEDS][GSH]^2} = \frac{(240)(480)^2}{(1760)(1520)^2} = 1.36 \times 10^{-2}$$

below. From this value of $E°$, the redox potential for HEDS can

$$\Delta G = -RT \ln K_{eq} = -(1.99\ cal/(mol\cdot deg))\ (4.18\ J/cal)\ (303\ K)\ (-4.30)$$

$$\Delta G° = 10\,840\ J/mol$$

$$E° = \frac{\Delta G°}{-nF} = \frac{10\,840}{(2)(96\,500)} = -0.06\ V$$

be estimated by difference from the standard value for GSH. [The

HEDS + $2e^-$ + $2H^+$ ⇌ 2β-ME	−0.29 V calcd by difference
2GSH ⇌ GSSG + $2e^-$ + $2H^+$	+0.23 V std value
HEDS + 2GSH ⇌ 2β-ME + GSSG	−0.06 V calcd from K_{eq} (above)

value of +0.23 V for the standard GSH/GSSG value is at pH 7 and unit activity of all other components relative to a standard hydrogen electrode of $[H^+] = 10^{-7}$ M in an ideal solution (from Marshall (1978)).]

Scheme I

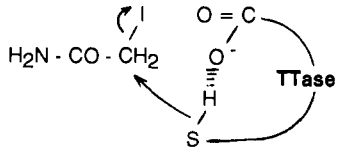

1980). This pK_a is almost 2 pH units below the normal value of about pH 8.5 for solvent-exposed protein thiols (Lindley, 1960), but it is near the pH optimum of 7.4 for the protein disulfide reductase activity of thioredoxin (Kallis & Holmgren, 1980). Thus, ionization of the active-site thiol of thioredoxin could participate in the rate-limiting step of catalysis by this enzyme, and it might be influenced differently by different substrates. The basis for the low pK_a of Cys-32 was challenged recently, however, when mutagenic replacement of the neighboring lysine cation with anionic glutamate was reported not to alter the pH dependence of thioredoxin activity (Gleason et al., 1990). This result suggests either that some other cation(s) stabilize(s) the thiolate species on thioredoxin or that the reaction of the thiolate anion with the oxidized substrate is not involved in the rate-determining step(s). Support for the former explanation can be found in high-resolution X-ray data suggesting that other residues besides the mutated Lys may contribute to a cationic environment around the Cys-32 residue of *E. coli* thioredoxin (Katti et al., 1990). The latter explanation (i.e., that the Cys thiolate reaction may not be involved in the rate-limiting step) seems to apply more aptly to the TTase (glutaredoxin) enzymes that differ substantially from thioredoxin in several ways. In this context, our data for HRBC TTase (Figure 2) and the data of Gan and Wells (1987) for pig liver TTase contrast sharply with the thioredoxin data described above. In studies analogous to those with thioredoxin, the pH profile of iodoacetate inactivation of pig liver TTase was interpreted to correspond to deprotonation of Cys-22 SH with a pK_a of 2.5; in a later article the pK_a value was revised to pH 3.8 (Yang & Wells, 1990a). Not only does this value contrast with the corresponding value for thioredoxin, but also it differs greatly from the pH optimum for activity of the pig liver TTase, i.e., pH 8.5 (Yang & Wells, 1990a). Our studies with HRBC TTase indicated a pK_a of 3.5 for IAA inactivation (Figure 2), which is comparable to the revised value of 3.8 given for the pig liver enzyme. In contrast, titration of the catalytic reaction gave an apparent pK_a near 8.0 (Figure 2, inset). It is conceivable that the extremely low pK_a for the IAA inactivation process might reflect a hydrophobically shielded thiolate–cationic pairing. The lack of sensitivity of this pK_a value to changes in ionic strength over a 40-fold range (Figure 2), however, suggests either that the vicinity of the active-site thiol is not freely accessible to solvent, or that an interaction other than ion pairing might be involved. Thus, the unusual pK_a for IAA inactivation of the TTases might be explained by Scheme I, in which a carboxylate moiety (typical pK_a near 3.5) would serve as a general base catalyst of the reaction between the active-site cysteine moiety and IAA, so that the thiol moiety would display the reactivity of a thiolate although it is formally protonated. The loss of IAA inhibitory reactivity at low pH would be explained in this case by protonation of the carboxylate moiety with pK_a 3.5 rather than actual titration of the thiolate moiety. Interactions analogous to that pictured above have been proposed to explain the unusual reactivity of the active-site thiol groups in cysteine proteases such as papain and ficin (Torchinsky, 1981). Moreover, unusual pH dependence of IAA alkylation of creatine kinase and insensitivity of the alkylation rate to changes in ionic strength were attributed to hydrogen bonding of the active-site thiol moiety as depicted in Scheme I (Watts & Rabin, 1962). An analogous participation of an aspartate carboxylate moiety in a proton-transfer relay involving His and the Ser OH is believed to be involved in nucleophilic activation of the serine hydroxyl moiety in serine proteases such as chymotrypsin (Blow, 1971; Hess, 1971). After this paper was submitted, a report appeared (Gan et al., 1990) of an unusually low pK_a (<pH 4) for IAA reaction with yeast TTase also, and an analogous H-bonding interaction was suggested. Irrespective of the actual molecular basis for activation of the thiol moiety of TTase, the effective pK_a for its reaction with IAA or with disulfide substrates is nearly 5 pH units below the pH optimum for catalysis of disulfide reduction. This means that some other pH-sensitive reaction(s) besides the initial reaction of enzyme and RSSR′ must be rate-limiting for the overall reaction. Since the reactions of GSH with disulfide moieties should be enhanced by deprotonation of the GSH, it seems likely that this event may contribute to the observed pH–rate profile for the overall reaction (Figure 2, inset).

Role of the Intramolecular Disulfide in Catalysis. Gan and Wells (1987) showed that pig liver TTase was converted by pretreatment with [^{14}C]cystine to a form that was resistant to IAA inactivation but no radiolabel from the cystine was associated with the resistant enzyme after dialysis. This result is consistent with a stable intramolecular disulfide form of the TTase enzyme. Analogous results were reported earlier for rat liver TTase treated with [^{35}S]GSSG except that a form of the enzyme containing radiolabel was also isolated (E-S-^{35}S-G) besides the intramolecular disulfide form (Eriksson et al., 1974). In each case the isolated oxidized forms of the respective TTase enzymes were found to be fully active when recombined with GSH and oxidized substrates. Thus, the isolated oxidized forms were chemically competent to enter the catalytic cycle, but single-turnover studies were not performed to test their kinetic competence. In fact, in an earlier study Gan and Wells (1986) reported that pretreatment of rat liver TTase with disulfides inhibited the enzyme. The concept of a simple ping-pong mechanism with oscillation between the fully reduced and the intramolecular disulfide forms of the TTase active site is mechanistically satisfying in its chemical simplicity. Such a mechanism may apply to the thioredoxin system when thioredoxin reductase acts as the direct reducing agent for oxidized thioredoxin, unless the thioredoxin–thioredoxin reductase complex acts as a unit throughout the reaction sequence. With respect to the TTase (glutaredoxin) enzymes that utilize GSH as the direct reducing agent, however, our two substrate kinetic findings for the HRBC and rat liver TTases (intersecting lines; Figures 3 and 4) do not fit the simple ping-pong mechanism described; otherwise parallel lines would have been observed. Another observation that is inconsistent with the ping-pong scheme was reported recently in preliminary form. Although mutagenesis of pig liver TTase Cys-22 → Ser abolished activity, Cys-25 → Ser mutation did not, according to assays of cell extracts in which the mutant proteins were expressed (Yang & Wells, 1990b). This result would suggest either that the TTase can operate without forming an intermediate intramolecular disulfide or that bound GSH or one of the other Cys residues (Cys-78 or -82) might substitute for Cys-25. Clearly, further study on the mechanism of TTase catalysis is needed.

We propose an alternative mechanism (Figure 6) as a working hypothesis for additional study. According to this scheme, either GSH or the disulfide substrate (RSSR′) could interact first with the reduced enzyme, but bond-breaking/

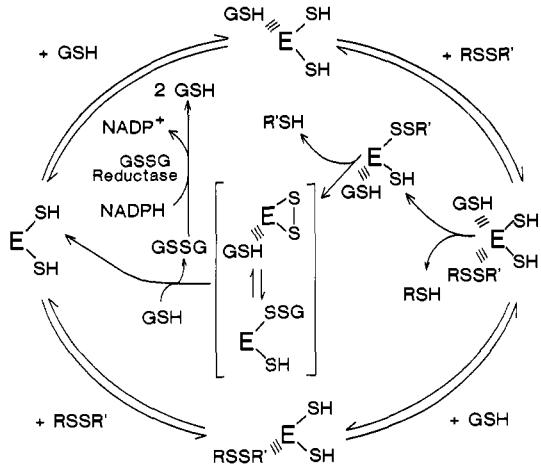

FIGURE 6: Hypothetical sequential mechanism for thioltransferase action. This scheme depicts a reaction mechanism whereby the reduced TTase enzyme interacts with both GSH and the oxidized substrate before releasing the reduced products of the oxidized substrate and regenerating the reduced enzyme. The intramolecular disulfide form of the enzyme may or may not be a kinetically important intermediate in the reaction mechanism.

making events leading to release of the reduced products (RSH and R'SH) would not occur until after the second substrate was bound. Whether or not an intramolecular disulfide form of the enzyme (shown in equilibrium with an alternative form) is a productive intermediate in the catalytic mechanism remains to be tested as alluded to above. The random mechanism shown in Figure 6 could be distinguished kinetically from an ordered mechanism, e.g., where GSH would be required to bind first, by using alternative substrates and product inhibitors [e.g., Huang (1977) and Chen, et al. (1988)]. Because the overall reaction is first order with respect to GSH concentration rather than second order (Figures 3 and 4), one of the two reactions shown for GSH must occur at a rate much faster than that of the other (Figure 6). Our further investigation will be aimed at unraveling the details of the GSH participation in the TTase catalytic mechanism, i.e., the feature that distinguishes TTases (glutaredoxins) from the closely related thioredoxin enzymes.

Role of GSSG Reductase in Net Disulfide Reduction by GSH and Thioltransferase (Glutaredoxin). In reports on the properties of the glutaredoxin enzymes from *E. coli* and calf thymus, Holmgren (1979, 1985b) stated that glutaredoxin-catalyzed ribonucleotide reductase activity (dCDP formation) was much slower in the absence of GSSG reductase; additions of GSSG were reported to inhibit the reaction further so that at a 1:1 ratio of GSH/GSSG no dCDP was formed during the standard 20-min incubation period. Presentation in this manner with a single time point makes it difficult to distinguish whether the diminution in product formation represented a decrease in the rate of the glutaredoxin-catalyzed reaction or an end point governed by the GSH/GSSG equilibrium. On the premise that this behavior might be a general property of the reactions catalyzed by glutaredoxin-like enzymes, we examined the GSH-dependent HRBC TTase-catalyzed reduction of the prototype substrates HEDS and cystine in the absence and presence of GSSG reductase in comparison to the non-TTase-catalyzed spontaneous reactions of these substrates with GSH (Table II and Figure 5). The initial rates of GSSG formation (NADPH equivalents) were similar in the absence and presence of GSSG reductase (Table II), and the extent of GSSG formation was essentially the same in the absence or presence of TTase, although TTase did accelerate the approach to the end point as expected (Figure 5). We interpret these results to reflect an equilibrium phenomenon rather than an inhibition of the TTase (glutaredoxin) enzyme by GSSG. For example, from the data of Figure 5 we can estimate an apparent redox potential for HEDS of −0.29 V relative to the standard redox potential of GSH at pH 7 (Marshall, 1978).

A striking feature of the above equilibrium data is the limitation on net reduction that can be accomplished by TTase in the absence of the coupled action of GSSG reductase. For example, with GSSG reductase and unlimited NADPH, the amount of TTase present in the experiments shown in Figure 5 would have catalyzed the reduction of more than 500 nmol of disulfide substrate (HEDS) in 60 min, rather than the 175 nmol observed. Projecting this relationship to the in vivo situation suggests that the net effect of TTase intracellularly could be governed by the activity of GSSG reductase and the NADPH-regenerating capacity of the respective cells. Thus, an intimate linkage among thioltransferase, GSSG reductase, and glucose-6-phosphate dehydrogenase might control intracellular sulfhydryl homeostasis, and interference with more than one of these three enzymes could have synergistic deleterious effects (Mieyal et al., 1991).

Acknowledgments

We are grateful to Drs. Dennis Koop, Michael Maguire, and Leslie Webster, Jr., for critical review of the manuscript before submission. We also thank Dr. Hesham El Messeery for technical assistance.

References

Blow, D. M. (1971) in *Enzymes (3rd Ed.)* (Boyer, P. D., Ed.) Vol. 3, pp 185–212, Academic Press, New York.
Caceci, M. S., & Cacheris, W. P. (1984) *Byte 9*, 340–362.
Chen, W.-J., Graminski, G. F., & Armstrong, R. A. (1988) *Biochemistry 27*, 647–654.
Eriksson, S., Askelof, P., Axelsson, K., & Mannervik, B. (1974) *Acta Chem. Scand., Ser. B 28*, 931–936.
Flohe, L., & Gunzler, W. A. (1974) in *Glutathione, Proc. Conf. Ger. Soc. Biol. Chem., 16th, 1973*, pp 132–144.
Gan, Z., & Wells, W. (1986) *J. Biol. Chem. 261*, 996–1001.
Gan, Z., & Wells, W. (1987) *J. Biol. Chem. 262*, 6704–6707.
Gan, Z., Sardana, M. K., Jacobs, J. W., & Polokoff, M. A. (1990) *Arch. Biochem. Biophys. 282*, 110–115.
Gleason, F. K., Lin, C-J., Gerami-Nejad, M., & Fuchs, J. A. (1990) *Biochemistry 29*, 3701–3709.
Guengerich, F. P. (1990) *CRC Crit. Rev. Biochem. Mol. Biol. 25*, 97–153.
Hess, G. P. (1971) in *Enzymes (3rd Ed.)* (Boyer, P. D., Ed.) Vol. 3, pp 213–248, Academic Press, New York.
Holmgren, A. (1979) *J. Biol. Chem. 254*, 3672–3678.
Holmgren, A. (1985a) *Annu. Rev. Biochem. 54*, 237–271.
Holmgren, A. (1985b) *Methods Enzymol. 113*, 525–540.
Holmgren, A. (1989) *J. Biol. Chem. 264*, 13963–13966.
Huang, C. Y. (1977) *Arch. Biochem. Biophys. 184*, 488–495.
Kallis, G.-B., & Holmgren, A. (1980) *J. Biol. Chem. 255*, 10261–10265.
Katti, S. K., LeMaster, D. M., & Ecklund, H. (1990) *J. Mol. Chem. 212*, 167–184.
Kitz, R., & Wilson, I. B. (1962) *J. Biol. Chem. 237*, 3245–3249.
Lindley, H. (1960) *Biochem. J. 74*, 577–584.
Mannervik, B., Axelsson, K., Sundewall, A., & Holmgren, A. (1983) *Biochem. J. 213*, 519–523.
Mannervik, B., Carlberg, I., & Larson, K. (1989) in *Coenzymes and Cofactors* (Dolphin, D., Paulson, R., Amramovic, O., Eds.) Vol III, Part A, Chapter 12, pp 475–516, John Wiley & Sons, New York.

Marshall, A. G. (1978) *Biophysical Chemistry: Principles, Techniques, and Applications*, pp 111–130, John Wiley & Sons, New York.
Mieyal, J. J., Starke, D. W., Gravina, S. A., Dothey, C., & Chung, J. (1991) *Biochemistry 30*, 6088–6097.
Papayannopoulos, I. A., Gan, Z., Wells, W. W., & Biemann, K. (1989) *Biochem. Biophys. Res. Commun. 159*, 1448–1454.
Park, E. M. & Thomas, J. A. (1989) *Arch. Biochem. Biophys.*, *272*, 25–31.
Segel, I., & Johnson, M. (1963) *Anal. Biochem. 5*, 330–337.
Stryer, L., Holmgren, A., & Reichard, P. (1967) *Biochemistry 6*, 1016–1020.
Torchinsky, Y. M. (1981) *Sulfur in Proteins*, pp 133–142, Pergamon Press, New York.
Watts, D. C., & Rabin, B. R. (1962) *Biochem. J. 85*, 507–516.
Yang, Y., & Wells, W. W. (1990a) *J. Biol. Chem. 265*, 589–593.
Yang, Y., & Wells, W. W. (1990b) *FASEB J. 4*, A2118.
Ziegler, D. M. (1985) *Annu. Rev. Biochem. 54*, 305–329.

Structure–Function Relationships in Human Epidermal Growth Factor Studied by Site-Directed Mutagenesis and ^{1}H NMR†

Ulrich Hommel,‡ Timothy J. Dudgeon,‡,§ Anthony Fallon,§ R. Mark Edwards,§ and Iain D. Campbell*,‡
Department of Biochemistry, University of Oxford, South Parks Road, Oxford OX1 3QU, U.K., and British Biotechnology Ltd., Thames Court, Watlington Road, Oxford OX4 5LY, U.K.

Received April 8, 1991; Revised Manuscript Received June 12, 1991

ABSTRACT: In order to elucidate the mechanism of interaction between human epidermal growth factor (EGF) and its receptor, selected variants of EGF, differing by single amino acid substitutions, have been made by site-directed mutagenesis. The receptor affinity of these mutants was determined by a receptor binding competition assay, and the effects of the substitution on the structure of the protein were assessed by ^{1}H nuclear magnetic resonance techniques. Various substitutions of Arg-41 resulted in substantial reduction in receptor affinity of EGF whereas change of Tyr-13 did not affect binding to the receptor. The ^{1}H resonances of all nonexchangeable protons of the Tyr-13 → Leu, Arg-41 → His, and Leu-47 → Glu variants were assigned and compared in order to assess the structural integrity of these mutants, which possess very different spectral and biological properties. In the case of the Leu-47 → Glu mutant, only minor localized spectral changes were observed, confirming that the tertiary structure of the protein is preserved upon mutation. In contrast, for both the Arg-41 → His and Tyr-13 → Leu variants, significant and strikingly similar spectra changes were observed for many residues located far away from the mutated residues. This implies that similar structural alterations have taken place in both proteins, an idea further supported by hydrogen-exchange experiments where the exchange rates of hydrogen-bonded amide protons for both the Tyr-13 → Leu and the Arg-41 → His mutants were found to be about 4 times faster than in the wild-type protein. Nuclear Overhauser enhancements, indicating specific structural features of hEGF, were measured for all mutants to ascertain that gross structural changes have not occurred. A structural model is proposed, to explain the observed effects brought about by the mutations Arg-41 → His and Tyr-13 → Leu.

Human epidermal growth factor is a 53 amino acid protein that stimulates mitogenesis by activating the tyrosine kinase domain of a cell-surface receptor (Carpenter et al., 1978; Ushiro & Cohen, 1980; Ullrich & Schlessinger, 1990). Several other proteins are homologous to EGF,[1] and they are believed to activate the EGF receptor in a way similar to that of EGF by ligand-induced oligomerization of the receptor (Yarden & Schlessinger, 1987). Human TGFα, for example, competes with EGF for the EGF receptor and has properties similar to those of EGF (Derynck et al., 1984; DeLarco & Todaro, 1980). Three members of the Pox virus family also possess EGF homologous sequences, and in some cases these proteins have been shown to bind to the EGF receptor (Lin et al., 1988; Upton et al., 1987; Twardzik et al., 1985). Cell growth promoting activities have also been found for other proteins containing EGF-like sequences such as amphiregulin (Shoyab et al., 1989), heparin binding growth factor (Higashiyama et al., 1991), and fragments of laminin (Panayotou et al., 1989).

Considerable progress has been made recently in understanding the basis for the recognition of EGF by its receptor. The three-dimensional structure of mouse EGF and that of a biologically active derivative, human EGF(1–48), have been determined by a combination of high-resolution ^{1}H NMR and computational techniques (Cooke et al., 1987; Montelione et al., 1987). In addition, the secondary structure of rat EGF (Mayo et al., 1989) and various three-dimensional structures of human TGFα have also been reported (Kohda et al., 1989; Kline et al., 1990; Harvey et al., 1991). This structural knowledge and the information available from the comparison of amino acid sequences of proteins with growth factor activity

† Financial support by EMBO to U.H. is gratefully acknowledged. This is a contribution from the Oxford Centre for Molecular Sciences, which is supported by the Science and Engineering Research Council and the Medical Research Council.
* Author to whom correspondence should be addressed.
‡ University of Oxford.
§ British Biotechnology Ltd.

[1] Abbreviations: ACN, acetonitrile; COSY, correlated spectroscopy; DQF-COSY, double-quantum filtered COSY; hEGF, human epidermal growth factor; NMR, nuclear magnetic resonance; NOESY, nuclear Overhauser spectroscopy; hTGF, human transforming growth factor; RP-HPLC, reversed-phase high-performance liquid chromatography; SDS–PAGE, sodium dodecyl sulfate–polyacrylamide gel electrophoresis; TFA, trifluoroacetic acid.

0006-2960/91/0430-8891$02.50/0